A5 - Structure Solution from Powder Diffraction Data - Applications I

A5 - O1

MOLECULAR CRYSTAL STRUCTURES FROM POWDER X-RAY DIFFRACTION TECHNIQUES

Eugene Y. Cheung, Andrew J. Hanson, Scott Habershon, Fang Guo, and Kenneth D.M. Harris

School of Chemistry, Cardiff University, PO Box 912, Cardiff CF10 3TB, UK
E-mail: eyc@struct.chem.cf.ac.uk

With the advances of direct space strategies for structure solution from powder X-ray data [1,2], and in particular the success of the Genetic Algorithm method [3,4], structural problems in a variety of fields are being tackled using information from powder data. Structural problems which have the complexity of more than one molecule in the asymmetric unit present new challenges to powder X-ray diffraction [5], and strategies to improve the probability of success in solving crystal structures are explored. Recent developments in the structure solution of complicated structures using powder diffraction techniques will also be highlighted.[6]

[1] Harris, K.D.M.; Tremayne, M.; Lightfoot, P.; Bruce, P.G. J. Am. Chem. Soc. 1994, 116, 3543.

[2] Harris, K.D.M.; Tremayne, M.; Kariuki, B.M. Angew. Chemie Int. Ed. 2001, 40, 1626.

[3] Harris, K.D.M.; Johnston, R.L.; Kariuki, B.M. Acta Crystallogr. 1998, A54, 632.

[4] Kariuki, B.M.; Serrano-González, H.; Johnston, R.L.; Harris, K.D.M. Chem. Phys. Lett. 1997, 280, 189.

[5] Cheung, E.Y.; Kitchin, S.J.; Harris, K.D.M.; Imai, Y.; Tajima, N.; Kuroda, R. 2003, 125, 14658.

[6] Cheung, E.Y.; Foxman, B.M.; Harris, K.D.M. Crystal Growth and Design. 2003, 3, 705.

A5 - O2

AB INITIO STRUCTURE DETERMINATION OF TWO ANHYDROUS FORMS OF -LACTOSE BY POWDER X-RAY DIFFRACTION

C. Platteau, J. Lefebvre, S. Hemon, F. Affouard, J.F. Willart and P. Derollez

Laboratoire de Dynamique et Structure des Matériaux Moléculaires (UMR CNRS 8024), Bâtiment P5, Université des Sciences et Technologies de Lille, 59655 Villeneuve d'Ascq Cédex, France.

Lactose, a milk sugar, fixes the molecules of water, which permits to increase the duration of preservation of a product. Consequently, lactose is of great interest for food and pharmaceutical industries. Lactose (4-O- -D-galactopyranosyl-D-glucopyranose), is a 'mixed' disaccharide containing a galactose and a glucose unit linked through a –1,4 linkage. It exhibits two anomers (–lactose and –lactose) which differ in the configuration of the terminal hydroxyl group of the glucose unit. For the –anomer, three crystalline forms have been characterised [1] : the –lactose monohydrate (hereafter named L-H_2O), the hygroscopic anhydrous –lactose (L_H) and the stable anhydrous –lactose (L_S). The –anomer has only one crystalline form (L); mixed compounds - -lactose have also been identified with different stoechiometries (/ L) [2], [3]. The crystalline structures of the L-H_2O form [4], [5], [6] and L form [7] were solved from single crystal samples with an automatic X-ray diffractometer.

The aim of this abstract is to explain the ab initio structure determination of two anhydrous forms of -lactose by powder X-ray diffraction: the L_H form and the stable anhydrous phase of –lactose. The reason why we did it on powder is given for each phase in the next parts. We have followed the same procedure for the two phases:

1) The data were collected on the laboratory diffractometer equipped with an INEL curved sensitive detector CPS120. A bent quartz monochromator allows to select the $K_{\alpha 1}$ wavelength of a Cu X-ray tube (= 1.54056 Å). The powder was introduced in a Lindemann glass capillary (diameter = 0.7mm), mounted on the axis of the diffractometer. It was rotated during the experiment in order to reduce the effect of possible preferential orientations.

2) The profiles of n reflections were individually refined with the program Winplotr [8] in order to obtain their exact 2 positions. We used then the program TREOR [9] to index the reflections. A part of the X-ray diffraction pattern was refined with the cell found by TREOR and using the "profile matching" option [10] of the program FullProf [11], in order to determine the space group.

3) Lattice and profile parameters, zero point and interpolated background calculated with the previous refinements were introduced in the program F.O.X. [12] in order

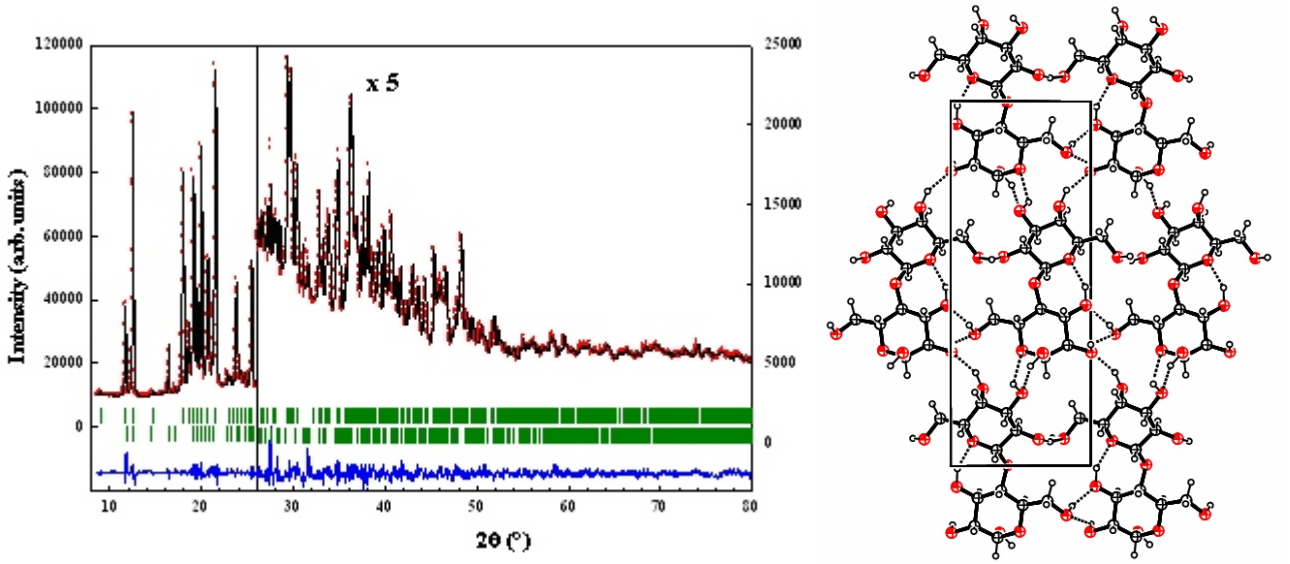

Figure 1: (a) Final Rietveld plot of the hygroscopic phase of -lactose. Observed data points are indicated by dots, the best-fit profile (upper trace) and the difference pattern (lower trace) are solid lines. The vertical bars correspond to the position of Bragg peaks: upper bars for L_H, lower bars for L-H_2O. **(b)** Projection of the unit cell of the hygroscopic -lactose along c*. Dashed lines correspond to H bonds.

to get a starting structural model. The "parallel tempering" algorithm of this program was used.

4) The final structure was obtained through Rietveld refinements with soft restraints on interatomic bond lengths and bond angles (program Fullprof [11]) and crystalline energy minimisation to locate the H atoms of the hydroxyl groups.

The results are the following :

1. the hygroscopic anhydrous phase of –lactose

-lactose monohydrate annealed at 135°C allowed to get *a mixture of this compound with hygroscopic anhydrous –lactose*. A powder X-ray diffraction pattern of this mixture was recorded at room temperature. To determine the lattice parameters of the phases, the profiles of the 58 reflections with a 2 angle lower than 40° were refined with the program Winplotr. Among the 58, 44 reflections were attributed to the L-H_2O form but 14 of them ranging from 9 to 33° do not belong, unambiguously, to the L-H_2O phase. Having isolated the L_H phase, we could continue the procedure as described beforehand. We have found a monoclinic symmetry, a space group $P2_1$ with 2 molecules per cell (Z' = 1), and the following lattice parameters: a = 7.7795 (3), b = 19.6931 (7), c = 4.9064 (1) Å, = 103.691 (2)°, V = 730.32 (4) Å^3. The final Rietveld plot is given on figure 1a (R_p = 0.0657, R_{wp} = 0.0733, R_{exp} = 0.0222, ^{2} = 10.9). The crystalline cohesion is achieved by networks of O–H···O hydrogen bonds (figure 1b). The

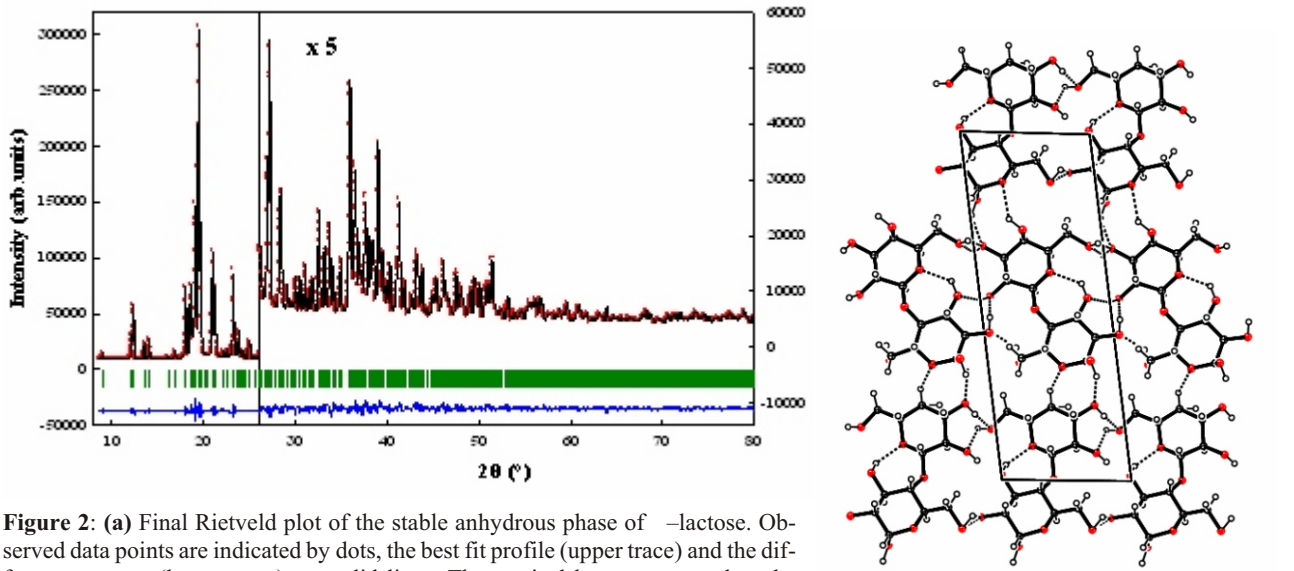

Figure 2: **(a)** Final Rietveld plot of the stable anhydrous phase of –lactose. Observed data points are indicated by dots, the best fit profile (upper trace) and the difference pattern (lower trace) are solid lines. The vertical bars correspond to the position of Bragg peaks. **(b)** Projection along c* of the unit cell of the stable anhydrous form of -lactose. Dashed lines correspond to H bonds.

width of the Bragg peaks is interpreted by a phenomenological microstructural approach in terms of isotropic size effects.

2. the stable anhydrous phase of –lactose

The stable anhydrous –lactose (L_S) form, not commercially available, can be obtained from L-H_2O either by heating at about 140°C or by dehydration in an hygroscopic solvent such as methanol [13], which we have used. To get single crystals to perform X-ray experiments with an automatic diffractometer, the L_S powder must be dissolved in a solvent and, then, crystals grow either by temperature lowering or by evaporation. In solution, the molecule of lactose can undergo hydration to form L-H_2O or mutarotation to form L. For this reason, the structure of the L_S form was solved *ab initio* from powder X-ray pattern using the Rietveld method. We have found a triclinic symmetry, a space group P1 with 2 molecules per cell, and the following lattice parameters: a = 7.6522 (2), b = 19.8637 (5), c = 4.9877 (1) Å, = 92.028 (1)°, = 106.261 (1)°, = 97.153 (1)°, V = 720.18 (4) Å^3. The final Rietveld plot is given on figure 2a. (R_p = 0.0555, R_{wp} = 0.0624, R_{exp} = 0.0159, ^{2} = 15.5). The crystalline cohesion is achieved by networks of O–H···O hydrogen bonds different to those of the L-H_2O and L_H phases (figure2b). The broadening of the Bragg reflections is interpreted in terms of size of the crystallites and of strain of the lattice.

[1] Garnier, S. (2001), Thesis, University of Rouen, (France).

[2] Burshill, J. H., Wright, W. B., Fuller, H. F. & Bell, A. V. (1965) *J. Sci. Food Agric.* 16, 622-628.

[3] Lerk, C. F., Andreae, A. C., Boer, A. H. de, Hoog, P. de, Kussendrager, K. & Leverink, J. van (1984). *J. Pharm. Sci*. **73**, 856-857.

[4] Fries, D. C., Rao, S. T. & Sundaralingam, M. (1971). *Acta Cryst*. **B27**, 994-1005.

[5] Beevers, C. A. & Hansen, H. N. (1971). *Acta Cryst*. **B27**, 1323-1325.

[6] Noordik, J. H., Beurskens, P. T., Bennema, P., Visser, R. A. & Gould, R. O. (1984). *Z. Kristallogr*. **168**, 59-65.

[7] Hirotsu, K. & Shimada, A. (1974). *Bull. Chem. Soc. Japan* **47**, 1872-1879.

[8] Roisnel, T. & Rodriguez-Carvajal, J. (2002). *Mater. Sci. Forum* **378-381**, 118-123.

[9] Werner, P. E., Eriksson, L. & Westdahl, M. (1985). *J. Appl. Cryst.* **18**, 367-370.

[10] Le Bail, A., Duroy, H. & Fourquet, J. L. (1988). *Mater. Res. Bull.* **23**, 447-452.

[11] Rodriguez-Carvajal, J. (2001). FullProf, version 1.9c, LLB, CEA/Saclay, France.

[12] Favre-Nicolin, V. & Cerny, R. (2002). *J. Appl. Cryst*. 35, 734-743. [8] Kreveld, A. van (1969). *Neth. Milk Dairy J*. **23**, 258-275.

[13] Kreveld, A. van (1969). *Neth. Milk Dairy J*. **23**, 258-275.

A5 - O3

CRYSTAL STRUCTURE OF GUAIFENESIN, 3-(2-METHOXYPHENOXY)-1,2-PROPANEDIOL

James A. Kaduk

P Chemicals, P.O. Box 3011 MC F-9, Naperville IL 60566, USA

The crystal structure of the common expectorant guaifenesin, 3-(2-methoxyphenoxy)-1,2-propanediol ($C_{10}H_{14}O_4$) was solved by applying Monte Carlo simulated annealing techniques to synchrotron powder data, and refined using the Rietveld method. Initial structure solutions yielded an unreasonable conformation, and an unacceptable refinement. Quantum chemical geometry optimizations were used to identify the correct conformation. Guaifenesin crystallizes in the orthorhombic space group $P2_12_12_1$ (#19), with a = 7.65705(7), b = 25.67020(24), c = 4.97966(4) Å, V = 978.79(2) Å^3, and Z = 4. Both hydroxyl groups act as hydrogen bond donors and acceptors, resulting in the formation of a 2-dimensional network of strong hydrogen bonds in the *ac* plane. The solid state conformation is ~4 kcal/mole higher in energy than the minimum-energy conformation of an isolated molecule, but the formation of the hydrogen bonds results in an energy gain of ~100 kcal/mole. Knowledge of the crystal structure permits quantitative phase analysis of guaifenesin-containing pharmaceuticals (such as Duratuss GP 120-1200) by the Rietveld method.

A5 - O4

DEHYDRATION IN ENVIRONMENTAL-FRIENDLY FLAME RETARDANTS. STRUCTURAL ANALYSIS OF MELAMINE PHOSPHATES USING X-RAY POWDER DIFFRACTION, SOLID STATE NMR AND AB INITIO CALCULATIONS

V. Brodski[1], D. J. A. De Ridder[1], R. Peschar[1], H. Schenk[1], A. Brinkmann[2], E. R. H. van Eck[2], A. P. M. Kentgens[2], B. Coussens[3] and Ad Braam[3]

[1]Universiteit van Amsterdam, Institute of Molecular Chemistry (IMC), Laboratory for Crystallography, Nieuwe Achtergracht 166, NL-1018WV Amsterdam, The Netherlands
[2]University of Nijmegen, Physical Chemistry / Solid State NMR, NSRIM Center, Toernooiveld 1, NL-6525 ED Nijmegen, The Netherlands
[3]DSM Research, Postbus 18, 6160 MD, Geleen, The Netherlands

Interest in melamine phosphates is high because they are attractive environmental-friendly alternatives to halogen-containing flame-retardants [1]. By combining information from three different techniques, X-ray powder diffraction, solid-state NMR and ab initio calculations, crystal structures of three melamine phosphates have been established: melamine orthophosphate [2], melamine pyrophosphate [3], and polymerized melamine phosphate [4]. The latter two arise as the result of dehydration processes that take place at elevated temperatures.

Crystal structure models were obtained on the basis of X-ray powder diffraction experiment using a newly developed Monte-Carlo approach [5]. The precise proton-bonding networks, crucial in the formation of the structures and the dehydration mechanism, are supported by ab initio energy minimizations and corroborated experimentally by solid-state NMR data.

The packing in the investigated compounds consists of infinite ribbons of melaminium cations crosslinked by chains of phosphate anions. Within the cation ribbons, adjacent melaminium moieties are linked by means of side-by-side pairs of N-H…N hydrogen bonds.

An analysis of the structural differences between the three melamine phosphates provides a first understanding of the underlying (de)hydration processes that are expected to play an important role in the flame-retardant activity of these materials.

Acknowledgement
The authors acknowledge the ESRF (Grenoble, France) for the opportunity to perform the synchrotron diffraction experiments and Dr. H. Emerich for his help at beamline BM01B (Swiss-Norwegian CRG). They also thank E.J. Sonneveld and Dr. M.M. Pop for their help in data collection and indexing, Dr. R.B. Helmholdt, Dr. V. M. Litvinov and Drs. K. Goubitz for useful discussions. This work was supported by DSM (Geleen, The Netherlands), Ciba Speciality Chemicals (Basel, Switzerland) and the Netherlands Foundation for Scientific Research (NWO).

[1] Sh. Jahromi, W. Gabriëlse, A. Braam, *Polymer* 44 (2003), 25-37.

[2] D. J. A. De Ridder, K. Goubitz, V. Brodski, R. Peschar, H. Schenk, *J. Mat. Chem.*, submitted.

[3] V. Brodski, R. Peschar, H. Schenk, A. Brinkmann, E. R. H. van Eck, A. P. M. Kentgens, B. Coussens, A. Braam, Angew. Chem., submitted.

[4] V. Brodski, R. Peschar, H. Schenk, A. Brinkmann, E. R. H. van Eck, A. P. M. Kentgens, B. Coussens, A. Braam, in manuscript.

[5] V. Brodski, R. Peschar, H. Schenk, J. Appl. Cryst. 36 (2003), 239-243.

A5 - O5

STRUCTURE AND STRUCTURE-RELATED ELECTROCHEMICAL PROPERTIES OF $Li_XMn_{2-X}Ti_XO_4$ (0.2 X 1.5) SPINELS

K. Petrov[1], R-M. Rojas[2], J-M. Rojo[2], J-M. Amarilla[2], M. G. Lazarraga[2], L. Pascual[2]

[1]*Institute of General and Inorganic Chemistry, Bulgarian Academy of Sciences, Acad. G. Bontchev street, bl 1, 1113 Sofia, Bulgaria*

[2]*Instituto de Ciencia de Materiales de Madrid, Consejo Superior de Investigaciones Cientificas, Cantoblanco, 28049 Madrid, Spain*

Series of lithium manganese titanium spinel-like oxides $LiMn_{2-x}Ti_xO_4$ ($0.2 < x$ 1.5) were synthesized and characterized by X-ray powder diffractometry, thermal analysis, EPR spectroscopy and electrochemical methods. Compounds whose composition falls within the interval $0.2 < x$ 1.0 crystallize in the space group Fd3m, whereas those having $x > 1.0$ crystallize in the space group $F4_332$. In some earlier studies it was claimed that the 8a sites in $LiMnTiO_4$ have mixed occupancies (Li0.75Ti0.25) [1, 2]. Data from XRD Rietveld structural refinement revealed that, in the whole compositional interval studied, the tetrahedral sites of the spinel-like structure are shared by Li^+ and Mn^{2+}, the partial occupancy of the latter increasing from 0.017 to 0.495 with increasing x from 0.2 to 1.5. The end member $LiMn_{0.5}Ti_{1.5}O_4$, synthesized in argon atmosphere, is reported for the first time. It crystallizes (see Table 1 and Table 2) in the cubic space group $F4_332$, a = 8.437 Å.

The refined positional parameters for $LiMn_{0.5}Ti_{1.5}O_4$ are in a good agreement with those reported earlier for several iso-structural spinel-like oxides with a general formula $Li_{1-y}M_y[(Li_yM_{0.5-y})\ M'_{1.5}]O_4$, (M = Mg, Co, Zn; M' = Ti; y 0.5) and (M = Co, Zn; M' = Ge; y 0.5). Refined site occupancies indicate clearly that Li and Mn atoms share the 8c tetrahedral sites with almost equal probability. Practically complete 1:3 ordering is observed in the octahedral (4b and 12d) sites, occupied by Li and Ti, respectively. The observed average metal-oxygen bond lengths are in excellent agreement with those calculated additively from the corresponding Shannon ionic radii. The values of the calculated BVS prove unambiguously that 4b and 12d sites are occupied exclusively by Li^+ and Ti^{4+}, correspondingly, supporting convincingly the validity of the refined structural model. The electrochemical performance in the 4 V region of the compounds used as cathode materials in lithium cells has been studied as a function of composition.

A gradual loss of capacity with increasing x from 0.2 to 0.8, followed by an abrupt fall at x = 1.0 was observed for the first charge. Charged samples undergo an irreversible phase transformation from spinel to defect rock-salt type structure, which explains the observed poor cycling behaviour after the first charge. Electrochemical data about charge/discharge capacities in the 3 V and 4V region have been used to estimate the Mn^{3+} content in the formula unit of the pristine cathode materials.

[1] B. Krutzsch and S. Kemmler-Sack, J. Less-Comm. Met., 124(1986)111-123.

[2] M. A. Arillo, M. L. López, M. T. Fernández, C. Pico, M. L. Veiga, A. Jiménez-López, E. Rodríguez-Castellon, J. Alloys and Compounds, 317-318(2001)160-163.

[3] Hiroo Kawai, Mitsuharu Tabuchi, Mikito Nagata, Hisashi Tukamoto and Anthony R. West, J. Mater. Chem, 8(5)(1998)1273-1280.

[4] V. S. Hernandez, L. M. T. Martinez, G. C. Mather and A. R. West, J. Mater. Chem., 6(1996)1533-1536.

Acknowledgements

The financial support of MECD, Spain, grant SAB: 2002-0002, is gratefully acknowledged by one of the authors (K. P.).

Table 1. Structural parameters of $LiMn_{0.5}Ti_{1.5}O_4$, space group $P4_332$, a = 8.4369(1) Å

Mn^{2+}	8c	0.0014(2)	0.0014(2)	0.0014(2)	0.65(5)	0.495(4)	R_{wp} = 0.131
Li^+	8c	0.0014(2)	0.0014(2)	0.0014(2)	0.65(5)	0.505(4)	R_p = 0.095
Ti^{4+}	12d	0.125*	0.3698(2)	0.8802(2)	0.66(3)	1.00	R_{exp} = 0.113
Mn^{3+},Mn^{4+}	4b	0.625	0.625	0.625	0.77(4)	0.010(4)	$\times^2$ = 1.38
Li^+	4b	0.625	0.625	0.625	0.77(4)	0.990(4)	GOF = 1.17
O^{2-}(1)	8c	0.3892(4)	0.3892(4)	0.3892(4)	1.13(7)	1.0	R_F = 0.027
O^{2-}(2)	24e	0.1032(5)	0.1266(5)	0.3909(5)	1.23(7)	1.0	R_B=0.038

Table 2. Selected tetrahedral (L_A)8c, average tetrahedral <L_A>, octahedral (L_B)4b, octahedral (L_B)12d and average octahedral - <L_B> bond lengths for $LiMn_{2-x}Ti_xO_4$ ($1.2 < x < 1.5$), space group $P4_332$.

x	L_A– O(1) (8c)	L_A– O(2) (8c)	<L_A> (8c)	L_B – O(2) (4b)	L_B – O(1) (12d)	L_B – O(2) (12d)	L_B –O(2) (12d)	<L_B>)
1.2	2.054(4)	1.996(3) 3	2.010	2.069(3)	2.010(3) 2	1.936(3) 2	1.985(3) 2	1.977
1.3	2.048(2)	2.002(2) 3	2.014	2.104(2)	2.022(2) 2	1.909(2) 2	1.983(2) 2	1.971
1.5	2.040(4)	2.010(4) 3	2.018	2.139(2)	2.041(2) 2	1.884(3) 2	1.984(2) 2	1.970

A5 - O6

STRUCTURE DETERMINATION AND REFINEMENT OF THREE NOVEL TERNARY PHASES IN THE Bi-Te-Ti-OXIDE SYSTEM

A. Meden[1], A. Kocevar[1], M. Udovic[2], M. Valant[2], D. Suvorov[2]

[1]Univ. of Ljubljana, Fac. of Chemistry & Chem. Tech., Askerceva 5, SI-1000 Ljubljana, Slovenia
[2]"Jozef Stefan" Institute, Jamova 39, Si-1000, Ljubljana, Slovenia

The ternary phase diagram of $Bi_2O_3 – TeO_2 – TiO_2$ was explored in order to locate possible candidates for use in the microwave wireless communication technology. Along with the desired microwave characteristics (appropriate dielectric constant, low dielectric loss, negligible temperature dependence of the resonant frequency), the possibility of sintering these materials at low temperatures was expected. This feature makes possible the use of the LTCC (Low Temperature Cofired Ceramics) technology where the whole module consisting of different ceramic electric elements (resistors, capacitors, conducting paths…) together with silver electrodes is assembled in green (pressed powder) state and sintered only once at the end.

All the phases of the corresponding binary systems, stable at room temperature in an oxygen atmosphere, were already known (four in $Bi_2O_3 – TeO_2$, four in $Bi_2O_3 – TiO_2$ and one in $TeO_2 – TiO_2$). This was, however, not the case for three ternary single phase materials with the expected compositions of $1Bi_2O_3$-$1TeO_2$-$1TiO_2$ (phase 1), $1Bi_2O_3$-$1TeO_2$-$3TiO_2$ (phase 2) and $2.5Bi_2O_3$-$1TeO_2$- $4TiO_2$ (phase 3) as determined by electron microscopy and X-ray powder diffraction. For none of them it was possible to find any structure with similar powder diffraction pattern in the PDF-2, so they were considered new structure types and subjected to an *ab-intio* SDPD.

Indexing with CRYSFIRE suite was successful in all three cases and eventually helped to subsequently purify the phase 1 (eliminate unindexed peaks). The unit cells were: monoclinic $a = 13.1$ Å, $b = 5.00$ Å, $c = 5.25$ Å and $= 108$ ° for phase 1, trigonal or hexagonal $a = 5.17$ Å and $c = 4.95$ Å for phase 2 and cubic $a = 9.40$ Å for phase 3.

At this point it was found by other methods, that during the synthesis in air, Te^{4+} was oxidized to Te^{6+}, so that TeO_3 should be expected in the above compositions. This means more oxygen and smaller Te^{6+} ion which can share the crystallographic sites with Ti^{4+}. This idea was used to put $(Te,Ti)O_6$ octahedra (Te : Ti ratio defined from the composition) and free Bi atoms into FOX. The number of each was varied to maintain the expected compositions, enable the occupation of special positions and satisfy the expected density (unit cell contents) for a selected space group. Several space groups were tested in each case and FOX gave reasonable solutions for all three phases. After the comparison of different solutions, the models in space groups P21/a, P-3 and Pn3 for phases 1, 2 and 3 respectively, were selected for the refinement.

Rietveld refinement using TOPAS was rather straightforward giving R_{wp} values between 10 and 12 % on the data from Bruker D4 diffractometer, Bragg-Brentano, CuK up to 2 of 140 °. Interatomic distances and coordinations were reasonable without using restraints. In all three cases it was confirmed that the Te and Ti atoms occupy the same sites and the refined population parameters were very close to the ones expected from the composition. The number of oxygen atoms in the structural models confirms the oxidation of Te^{4+} to Te^{6+} without doubt in the phases 1 and 2, which are octahedral frameworks consisting of edge-sharing BiO_6 (larger) and $(Te,Ti)O_6$ (smaller) octahedra. In the phase 3 there remain some doubts about the coordination around Bi, which is larger than 6, rather irregular and includes oxygen atoms which are not part of the octahedral framework. The number and positions of these extra-framework oxygen atoms and the cation composition (in the current model it differs from the proposed one) will have to be clarified in future (X-ray single crystal and neutron powder diffraction are possible alternatives).

All three phases are "small" structures, but despite that, show a range of difficulty from a routine (phase 2) through moderate (phase 1) to challenging (phase 3) and show the role of crystallographic thinking and use of complimentary techniques in the process of SDPD.